Novel Ni(0)-COT Complexes, Displaying Semiaromatic Planar COT Ligands with Alternating C−C and C═C Bonds†

Ingrid Bach, Klaus-Richard Pörschke,* Bernd Proft, Richard Goddard, Carsten Kopiske, Carl Krüger, Anna Rufińska, and Klaus Seevogel

Contribution from the Max-Planck-Institut für Kohlenforschung, Postfach 101353, D-45466 Mülheim an der Ruhr, Germany

Received December 6, 1996⊗

Abstract: Reaction of $(R_2PC_2H_4PR_2)Ni(C_2H_4)$ with COT gives the mononuclear complexes $(R_2PC_2H_4PR_2)Ni(\eta^2\text{-}C_8H_8)$ (R = ^{i}Pr **1a**, ^{t}Bu **1b**). The COT ligand in **1a,b** is planar with alternating C−C and C═C bonds, corresponding to a formal semiaromatic $[C_8H_8]^-$ ligand. Reactions of **1a** with $(^iPr_2PC_2H_4P^iPr_2)Ni(\eta^2,\eta^2\text{-}C_6H_{10})$ and of **1b** with stoichiometric amounts of $\{(^tBu_2PC_2H_4P^tBu_2)Ni\}_2(\mu\text{-}C_6H_6)$ or lithium afford the dinuclear complexes $\{(^iPr_2PC_2H_4P^iPr_2)Ni\}_2\{\mu\text{-}\eta^4(1,2,5,6):\eta^4(3,4,7,8)\text{-}C_8H_8\}$ (**2a**) and $\{(^tBu_2PC_2H_4P^tBu_2)Ni\}_2(\mu\text{-}\eta^2\text{:}\eta^2\text{-}C_8H_8)$ (**2b**; two isomers). The COT ligand in **2a** is tub-shaped and olefinic, whereas in **2b** (as in **1a,b**) it is planar and semiaromatic. The products are characterized by IR, solution and solid-state NMR spectroscopy, and by X-ray structure analysis.

Introduction

In the gas-phase[1] and in the crystal[2] neutral 8e cyclooctatetraene (COT, C_8H_8) displays a tub-shape conformation with alternating C═C (1.33 Å) and C−C (1.47 Å) bonds (D_{2d} symmetry). Ring inversion is likely to proceed through a planar transition state structure with the C−C bond length alternation maintained (D_{4h}); the energy of activation is estimated to be about 14 kcal mol^{-1}.[3] It has been proposed on the basis of vibronic modeling of the EPR spectrum[4] and ab initio calculations[5,6] that the 9e radical anion $[COT]^-$[7] in its ground-state is also of D_{4h} symmetry with a significant but reduced C−C bond length alternation of about 1.36 Å (C═C) and 1.44 Å (C−C) (1.359, 1.435 Å;[5] 1.375, 1.446 Å[6]). It has been further suggested that puckering and bond length alternation of the neutral COT is reduced by substituent electronic effects, an electron donor (methylene anion) being more effective than an electron acceptor (methylene cation). Spanning either the COT single or double bonds by fused-ring substitutions is also expected to promote the ring flattening.[6] A fully planar geometry and full equilibration of the C−C distances (1.41 Å) is attained for the 10e dianion $[COT]^{2-}$ (D_{8h}). It thus appears that with an increasing charge the COT ring gradually changes its properties from olefinic via semiaromatic ($[COT]^-$) to fully aromatic ($[COT]^{2-}$). By semiaromatic we mean here a planar ring with significant bond localization.

While there are numerous metal complexes with *olefinic nonplanar* COT ligands [e.g. $CpMn(CO)_2(\eta^2\text{-}C_8H_8)$ (tub-shaped *exo* coordinated COT ligand),[8] $(CO)_3Fe\{\eta^4(1\text{−}4)\text{-}C_8H_8\}$,[9] $[Ag\{\eta^4(1,2,5,6)\text{-}C_8H_8\}]NO_3$[10]] and *aromatic planar* COT ligands (e.g. $K_2[C_8H_8]$,[11] $U(\eta^8\text{-}C_8H_8)_2$[12]), apparently only one complex containing a *semiaromatic planar* COT ligand, dark red $Cp_2Ta(n\text{-}C_3H_7)(\eta^2\text{-}C_8H_8)$,[13] has been described. We now wish to report the preparation, spectroscopic, and structural characterization of a series of mono- and dinuclear complexes $(R_2PC_2H_4PR_2)Ni(\eta^2\text{-}C_8H_8)$ (R = ^{i}Pr **1a**, ^{t}Bu **1b**) and $\{(R_2PC_2H_4PR_2)Ni\}_2(\mu\text{-}C_8H_8)$ (R = ^{i}Pr **2a**, ^{t}Bu **2b**).[14] In **1a,b** and **2b** the COT ligand is also semiaromatic, whereas in **2a** it is olefinic.

Results

We have recently described a series of $[(d^ippe)Ni(0)]$[15] and $[(d^tbpe)Ni(0)]$[16,17] complexes with alkene, alkyne, and benzene ligands. These complex fragments combine an exceedingly bulky chelating phosphine ligand with the smallest central atom of the group 10 series Ni, Pd, Pt, resulting in a considerable steric effect at the metal. Unusual coordination properties of the metal have been observed, particularly for $[(d^tbpe)Ni(0)]$. For example, while $[(d^ippe)Ni(0)]$ forms trigonal-planar (*TP*-3) *or* tetrahedral (*T*-4) complexes with alkenes [e.g., 16e $(d^ippe)Ni(C_2H_4)$ *vs* 18e $(d^ippe)Ni(\eta^2,\eta^2\text{-}C_6H_{10})$, $(d^ippe)Ni(\eta^2,\eta^2\text{-}$

† Abbreviations: COT, cyclooctatetraene; d^ippe, $^iPr_2PC_2H_4P^iPr_2$, bis(di-isopropylphosphino)ethane; d^tbpe, $^tBu_2PC_2H_4P^tBu_2$, bis(di-*tert*-butylphosphino)ethane; NQS, nonquaternary supression.

⊗ Abstract published in *Advance ACS Abstracts,* March 15, 1997.

(1) Bastiansen, O.; Hedberg, L.; Hedberg, K. *J. Chem. Phys.* **1957**, *27*, 1311.

(2) Claus, K. H.; Krüger, C. *Acta Crystallogr. C* **1988**, *44*, 1632, and references cited therein.

(3) (a) Anet, F. A. L.; Bourn, A. J. R.; Lin, Y. S. *J. Am. Chem. Soc.* **1964**, *86*, 3576. (b) Oth, J. F. M. *Pure Appl. Chem.* **1971**, *25*, 573. (c) Hrovat, D. A.; Borden, W. T. *J. Am. Chem. Soc.* **1992**, *14*, 5879. (d) Paquette, L. A. *Acc. Chem. Res.* **1993**, *26*, 57.

(4) McLachlan, A. D.; Snyder, L. C. *J. Chem. Phys.* **1962**, *36*, 1159.

(5) Hammons, J. H.; Hrovat, D. A.; Borden, W. T. *J. Am. Chem. Soc.* **1991**, *113*, 4500.

(6) Trindle, C.; Wolfskill, T. *J. Org. Chem.* **1991**, *56*, 5426.

(7) Gebicki, J.; Michl, J. *J. Phys. Chem.* **1988**, *92*, 6452. Wenthold, P. G.; Hrovat, D. A.; Borden, W. T.; Lineberger, W. C. *Science* **1996**, *272*, 1456.

(8) Benson, I. B.; Knox, S. A. R.; Stansfield, R. F. D.; Woodward, P. *J. Chem. Soc., Chem. Commun.* **1977**, 404; *J. Chem. Soc., Dalton Trans.* **1981**, 51.

(9) Dickens, B.; Lipscomb, W. N. *J. Chem. Phys.* **1962**, *37*, 2084.

(10) (a) Mathews, F. S.; Lipscomb, W. N. *J. Phys. Chem.* **1959**, *63*, 845. (b) Ho, W. C.; Mak, T. C. W. *J. Organomet. Chem.* **1983**, *241*, 131.

(11) (a) Noordik, J. H.; van den Hark, T. E. M.; Mooij, J. J.; Klaassen, A. A. K. *Acta Crystallogr. B* **1974**, *30*, 833. (b) Hu, N.; Gong, L.; Jin, Z.; Chen, W. *J. Organomet. Chem.* **1988**, *352*, 61.

(12) Streitwieser, A.; Müller-Westerhoff, U. *J. Am. Chem. Soc.* **1968**, *90*, 7364. Zalkin, A.; Raymond, K. N. *J. Am. Chem. Soc.* **1969**, *91*, 5667.

(13) van Bolhuis, F.; Klazinga, A. H.; Teuben, J. H. *J. Organomet. Chem.* **1981**, *206*, 185. The reported NMR characterization of $Cp_2Ta(n\text{-}C_3H_7)(\eta^2\text{-}C_8H_8)$ is erroneous. In the ^{13}C NMR spectrum the signal at δ_C = 105.5 with $J(CH)$ = 178 Hz, previously assigned to the COT ligand, is due to one of the Cp ligands (Teuben, J. H. Personal communication). For the chiral static structure of the complex (18e) eight COT proton and carbon resonances are expected.

(14) Bach, I. Dissertation, Universität Düsseldorf, 1996.

(15) Pörschke, K.-R. *Angew. Chem.* **1987**, *99*, 1321; *Angew. Chem., Int. Ed. Engl.* **1987**, *26*, 1288, and unpublished results.

(16) Pörschke, K.-R.; Pluta, C.; Proft, B.; Lutz, F.; Krüger, C. *Z. Naturforsch., B: Anorg. Chem., Org. Chem.* **1993**, *48*, 608.

(17) Bach, I.; Pörschke, K.-R.; Goddard, R.; Kopiske, C.; Krüger, C.; Rufińska, A.; Seevogel, K. *Organometallics* **1996**, *15*, 4959.

S0002-7863(96)04210-2 CCC: $14.00

C_8H_{12}) (C_6H_{10} = 1,5-hexadiene, C_8H_{12} = 1,5-cyclooctadiene)],[15] the nickel atom of [(d^{t}bpe)Ni(0)] has only been observed in a *TP*-3 coordination geometry [e.g., 16e (d^{t}bpe)Ni(η^2-C_6H_{10}), (d^{t}bpe)Ni(η^2-C_8H_{12})].[16]

(i Pr$_2$PC$_2$H$_4$P^{i}Pr$_2$)Ni(η^2-C$_8$H$_8$) (1a) and (t Bu$_2$PC$_2$H$_4$P^{t}Bu$_2$)-Ni(η^2-C$_8$H$_8$) (1b). The solid yellow complexes (d^{i}ppe)Ni(η^2,η^2-C_6H_{10}) and (d^{t}bpe)Ni(C_2H_4) slowly dissolve in neat COT (20 °C) to afford dark red solutions. After addition of diethyl ether the color changes to brown, and at −78 °C fine, almost black needles of **1a** (mp 168 °C) or bulky, bluish purple needles of **1b** (mp 218 °C) separate in about 80% yield (eq 1). The crystals show a characteristic blue-purple metallic sheen. In the mass spectra the molecular ions (**1a**: *m/e* 424, 38%; **1b**: *m/e* 480, 14%) are observed, which fragment by cleavage of the COT ligand to afford the basis ions [(d^{i}ppe)Ni]$^+$ and [(d^{t}bpe)Ni]$^+$. In the IR spectrum (KBr) **1a** exhibits a visible[18] =C−H stretching band at 2999 cm^{-1} and two stretching bands for uncoordinated C=C bonds at 1591(s) and 1533(vs) cm^{-1}, while a stretching band at 1485(w) cm^{-1} is assigned to the coordinated C=C bond. For **1b** the =C−H stretching band appears at a somewhat lower wavenumber (2996 cm^{-1}) and the corresponding C=C vibrations are at higher wavenumbers [1602(s), 1553(vs), 1490(w, shoulder) cm^{-1}] than for **1a**. This pattern of absorption bands in the ring-stretching region, which was also observed for $Cp_2Ta(n\text{-}C_3H_7)(\eta^2\text{-}C_8H_8)$ [1595(s), 1515(vs), 1470(w)],[13] is characteristic of the planar η^2-C_8H_8 ligand, whereas the absorption band patterns of uncoordinated COT [3004(vs), 1635(s), 1609(m) cm^{-1}][19] and of K_2COT [2994(m), 1431(w), 880(s), 684(vs) cm^{-1}][20] are quite different.[21] Complexes **1a,b** are quite soluble in THF, even at low-temperature, but less so in pentane or diethyl ether (20 °C). The red brown solutions are stable for several weeks. According to NMR no fast exchange of coordinated and added COT occurs.

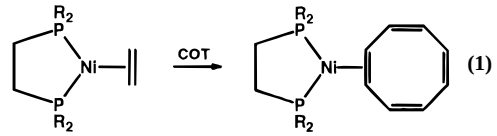

(1)

1a: R = ^{i}Pr
1b: R = ^{t}Bu

Solution NMR Spectra of 1a,b. The solution ^{1}H (400 MHz) and ^{13}C (75.5 MHz) NMR spectra of **1a,b** are well resolved at 27 °C, at which temperature the COT ligands gives rise to narrow triplets due to spin−spin couplings with the phosphorus atoms (Table 1). The COT ligand ^{1}H and ^{13}C resonances are at higher field than for uncoordinated COT, the ^{13}C chemical shift (**1a**: δ_C 103.4; **1b**: δ_C 106.5) being intermediate between that of uncoordinated COT (132.7) and of K_2COT (89.9). Correspondingly, the COT ligand coupling constants ^1J(CH) (**1a**: 149.7 Hz; **1b**: 148.8 Hz) are smaller than in the uncoordinated COT (154.5 Hz) but not as small as in K_2COT (143.4 Hz). The ambient temperature NMR spectra obviously represent the time average of a dynamic structure since a η^2-C_8H_8 coordination mode has been determined for **1a,b** in the crystal (see below). At −80 °C the COT ^{1}H and ^{13}C resonances of **1a** are just slightly broadened, whereas those of **1b** are markedly so; nevertheless the limiting spectra of the static structure of **1b** have not been observed down to −100 °C. The ^{31}P NMR spectra (27/−100 °C) of **1a,b** exhibit sharp singlets, which are for **1a** (δ_P 81.7) at distinctly lower field than for the corresponding ethene complex (d^{i}ppe)Ni(C_2H_4) (δ_P 72.4) but for **1b** (δ_P 93.0) at the same field as for (d^{t}bpe)Ni(C_2H_4) (δ_P 92.7).

Table 1. Solution ^{1}H, ^{13}C NMR Data (COT Ligand) and ^{31}P NMR Data of **1a,b** and **2b** (Semiaromatic COT), **2a** (Olefinic COT), and of Reference Compounds[d]

	δ_H	δ_C	^1J(CH) [Hz]	δ_P
COT	5.72	132.7	154.5	
1a	4.62	103.4	149.7	81.7
	J(PH) 1.2	*J*(PC) 2.1		
1b	4.50	106.5	148.8	93.0
	J(PH) 1.6	*J*(PC) 2.2		
2b	4.32[b]	90.9[b]	147.0	79.1
Li_2COT	5.73	87.5	144.7	
K_2COT[a]	5.68	89.9	143.4	
{(RN=CHCH=NR)Ni}$_2$-(μ-η^4:η^4-COT)[c 33]	3.81	98.2	159	
2a	4.47	90.3	154.5	65.5
	J(PH) 3.4	*J*(PC) 3.0		

[a] −80 °C. [b] Couplings *J*(PH) and *J*(PC) are not observed. [c] R = C_6H_3-2,6-^{i}Pr$_2$. [d] Solvent THF-d_8, temperature 27 °C or as indicated. Coupling constants in Hz.

The temperature dependent ^{1}H and ^{13}C NMR spectra can be explained by an exchange of the coordinated and uncoordinated COT C=C bonds. Starting from an 16e *TP*-3 ground-state structure ($R_2PC_2H_4PR_2$)Ni{η^2(1,2)-C_8H_8}, coordination of a C=C bond *adjacent* to the already coordinated one gives rise to an 18e *T*-4 intermediate (or transition state) [($R_2PC_2H_4PR_2$)-Ni(η^4(1−4)-C_8H_8)]. Dissociation of the first coordinated C=C bond leads to recovery of 16e *TP*-3 **1a,b**. This is equivalent to a rotation of the η^2-COT ligand by 90° (Figure 1a). Repetition of these steps results in an equilibration of all C=C bonds. The exceedingly facile C=C bond exchange (for **1a** even more facile than for **1b**) is due to an energetically easily accessible η^4(1−4)-C_8H_8 coordination mode (low-energy process), for which a dynamic structure is characteristic.[22]

In addition, it is likely that at ambient temperature the coordinated COT C=C bond in *TP*-3 **1a,b** also exchanges with the *transannular* uncoordinated C=C bond via (equally 18e *T*-4) intermediates [($R_2PC_2H_4PR_2$)Ni{η^4(1,2,5,6)-C_8H_8}] (high-energy process) (Figure 1b). These intermediates correspond to the cyclooctadiene complexes (d^{i}ppe)Ni{η^4(1,2,5,6)-C_8H_{12}} (isolated) and [(d^{t}bpe)Ni{η^4(1,2,5,6)-C_8H_{12}}] (intermediate); the latter has been postulated for the C=C bond exchange process in (d^{t}bpe)Ni(η^2-C_8H_{12}).[16]

Complexes displaying η^2-COT ligands are rare. For the 18e d^6 complexes $CpMn(CO)_2(\eta^2\text{-}C_8H_8)$[8] (dec 75 °C) and [$CpFe(CO)_2(\eta^2\text{-}C_8H_8)$]$PF_6$[23] (not isolated; dec 0 °C) the η^2-COT coordination is static up to the decomposition temperatures of the complexes. However, the statement[24] that η^2-COT coordination is generally static is obviously incorrect. Nonisolated complexes cited as (dppf)Pd(η^2-C_8H_8) and (dppf)Pt(η^2-C_8H_8) [dppf = 1,1′-bis(diphenylphosphino)ferrocene] have not been characterized in detail.[25] The related complex (d^{i}ppe)Pt(0)(η^2-

(18) Further =C−H bands are likely to be obscured by bands of the phosphine ligand.

(19) (a) Lippincott, E. R.; Lord, R. C.; McDonald, R. S. *J. Am. Chem. Soc.* **1951**, *73*, 3370. (b) Perec, M. *Spectrochim. Acta, Part A* **1991**, *47*, 799.

(20) Fritz, H. P.; Keller, H. *Chem. Ber.* **1962**, *95*, 158.

(21) Unfortunately, no IR data has been reported for the olefinic (nonplanar) COT ligand in $CpMn(CO)_2(\eta^2\text{-}C_8H_8)$.[8]

(22) Cotton, F. A. In *Dynamic Nuclear Magnetic Resonance Spectroscopy* Jackman, L. M., Cotton, F. A., Eds.; Academic Press: New York, 1975; p 377.

(23) Cutler, A.; Ehntholt, D.; Giering, W. P.; Lennon, P.; Raghu, S.; Rosan, A.; Rosenblum, M.; Tancrede, J.; Wells, D. *J. Am. Chem. Soc.* **1976**, *98*, 3495.

(24) Lawless, M. S.; Marynick, D. S. *J. Am. Chem. Soc.* **1991**, *113*, 7513.

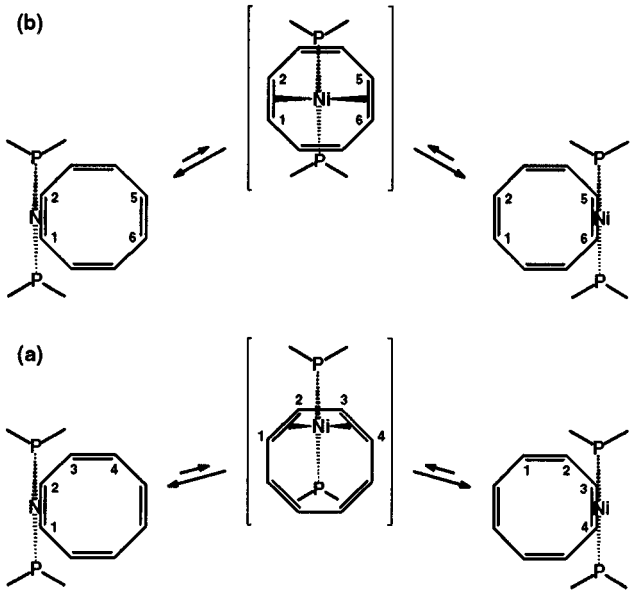

Figure 1. Suggested mechanisms for the exchange of coordinated and uncoordinated COT C═C bonds in **1a,b**: (a) low-energy process via a *T*-4-Ni(0)-η^4(1−4)-C_8H_8 intermediate (or transition state) and (b) high-energy process via a *T*-4-Ni(0)-η^4(1,2,5,6)-C_8H_8 intermediate (or transition state).

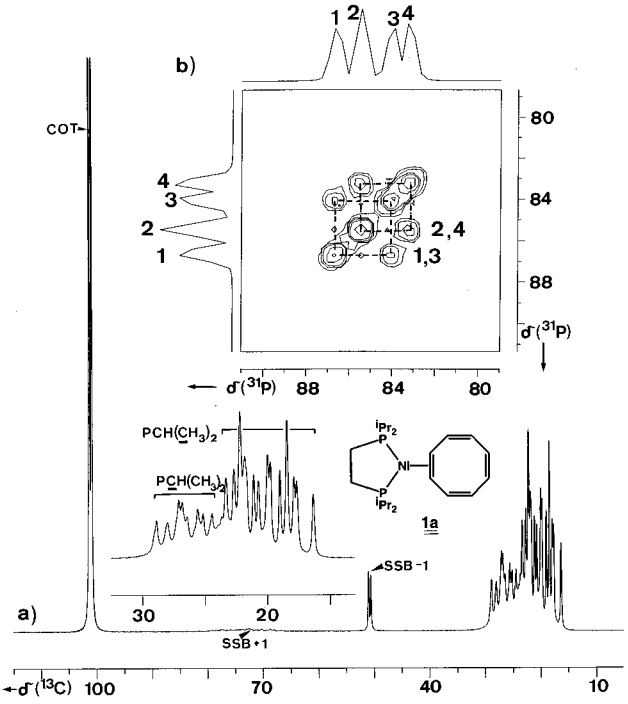

Figure 2. (a) ^{13}C CP-MAS NMR spectrum of **1a**. SSB±1: first spinning side-band to lower (−) or higher (+) frequency. (b) Isotropic part of 2D COSY ^{31}P CP-MAS NMR spectrum of **1a**. Signals 1 and 3 as well as signals 2 and 4 belong to two individual d^{i}ppe ligands (corresponding to two independent molecules of **1a** present in the asymmetric unit).

C_8H_8), recently synthesized by our group, is also fluxional, even as a solid at −100 °C (CP-MAS NMR). In solution this complex is in equilibrium with the isomer (d^{i}ppe)Pt(II)-{η^1(1),η^1(4)-C_8H_8}.[26]

Solid-State CP-MAS NMR Spectra of 1a,b. In addition to the solution NMR spectra we have studied the solid-state ^{13}C and ^{31}P CP-MAS NMR spectra (24 °C) of complexes **1a,b**. For the d^{i}ppe derivative **1a** (Figure 2a,b) the spectra display two sets of signals due to the presence of two independent C_1 symmetrical molecules in the asymmetric unit. The COT ligands give rise to two very sharp ^{13}C signals (δ_C 101.3 and 100.9) with a shift similar to that for the solution (δ_C 103.4). The equivalence of the eight ^{13}C nuclei of each COT ligand results from the fluxionality, which has been confirmed by a NQS ^{13}C NMR experiment. The independent d^{i}ppe ligands give rise to eight P*C*Me$_2$ signals (centered at δ_C 26.5) and 16 PC*Me*$_2$ signals (centered at δ_C 20.2), whereas the four signals expected for PCH_2 overlap. For the ^{31}P nuclei four signals are observed, corresponding to two unresolved AB spin systems (δ_P 86.6, 84.0 and δ_P 85.4, 83.3). For these, relatively small couplings J(PP) = 25 ± 5 and 28 ± 5 Hz, respectively, were determined by a *J*-resolved 2D ^{31}P NMR spectrum, while (due to the similar magnitude of the couplings) the assignment was made on the basis of a 2D COSY ^{31}P CP-MAS NMR spectrum (Figure 2b).

For the sterically more demanding d^{t}bpe derivative **1b**[27] the ^{13}C COT signal at δ_C 104.8 (solution NMR: δ_C 106.5) is rather broad. Although the dynamics of the COT ligand are obviously slower than for **1a**, it has not been possible to observe the limiting spectra of the static structure down to 85 K. The d^{t}bpe ligand gives rise to four P*C*Me$_3$ signals (δ_C 37.5, 37.2, 35.9, 35.4), three (of the expected four) PC*Me*$_3$ signals [δ_C 32.9 (two signals isochronous), 32.1, 31.3], and two PCH_2 signals (δ_C 25.6, 24.0). In the ^{31}P NMR spectrum two ^{31}P signals (δ_P 94.8, 94.0) are observed, for which the coupling J(PP) = 43 ± 5 Hz has been determined by *J*-resolved 2D ^{31}P NMR spectroscopy.

Thus, for both **1a,b** the COT ligands are fluxional in the solid-state and most likely the exchange of coordinated and uncoordinated C═C bonds proceeds as depicted in Figure 1a, since this involves the least motion of the COT ligand.

Molecular Structures of 1a,b. The structures of **1a,b** in the crystal have been determined by single-crystal X-ray structure analysis. In both complexes the Ni atom is trigonal-planar coordinated by two phosphorus atoms of the respective chelating d^{i}ppe and d^{t}bpe ligand and only one C═C bond of the COT ring.

The (d^{i}ppe)Ni complex **1a** (Figure 3) crystallizes with two independent molecules (C_1 point symmetry) in the asymmetric unit, which differ only in the arrangement at the isopropyl groups and to a lesser extent in the C_2 bridge. The geometries of the remaining atoms (Ni,P1,P2,C1−C8) in the two molecules are the same within experimental error (rms deviation 0.05 Å). In both cases the COT ring is planar (±0.1 Å) and coordinated by only one C═C bond to the Ni atom, with the ring plane bent only slightly away from the metal plane [Ni,C1,C2/(C1−C8) 93°]. Since the two independent molecules have perforce different environments, packing effects are an unlikely cause for the planarity of both the COT rings.

In spite of the planarity of the rings, the C−C bond distances in the uncoordinated part of the ring alternate [C═C_{mean} 1.36(4), C−C_{mean} 1.43(2) Å], while the C1−C2 bond [mean 1.407(4) Å] is lengthened by coordination to the metal. The bond length of the coordinated bond is similar to that of complexes containing a nonplanar C_8H_8 ligand. The bond length alternation in the uncoordinated part of the COT ligand is somewhat less than for uncoordinated nonplanar COT [C═C 1.33, C−C 1.47 Å] and agrees well with the alternation predicted for the planar monoanion COT^- [C═C 1.36, C−C 1.44 Å] (see Introduction).

(25) Brown, J. M.; Cooley, N. A. *Organometallics* **1990**, *9*, 353. Brown, J. M.; Pérez-Torrente, J. J.; Alcock, N. W.; Clase, H. J. *Organometallics* **1995**, *14*, 207.

(26) Haack, K.-J. Dissertation, Universität Düsseldorf, 1994.

(27) The solid-state ^{1}H MAS NMR spectrum of **1b**, although poorly resolved, displays for the COT ligand a broad singlet at δ_H 3.89 (solution NMR: δ_H 4.50).

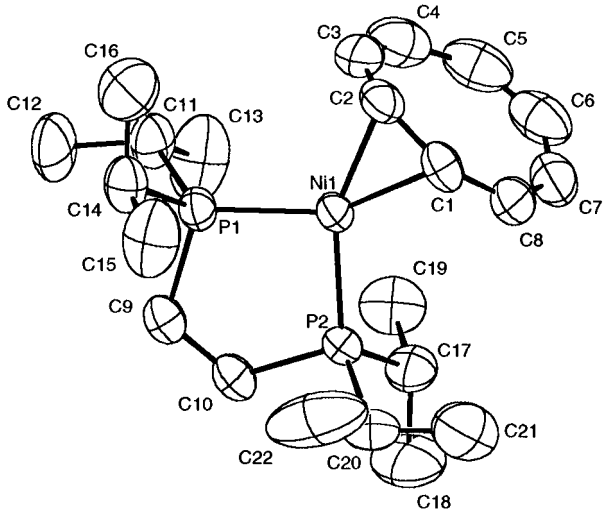

Figure 3. Molecular structure of complex **1a** (molecule 1). Selected bond distances (Å) and angles (deg) (average of two independent molecules): Ni1−P1 2.166(2), Ni1−P2 2.157(2), Ni1−C1 2.024(6), Ni1−C2 1.992(3), C1−C2 1.407(8), C2−C3 1.436(9), C3−C4 1.382(9), C4−C5 1.411(9), C5−C6 1.336(9), C6−C7 1.408(9), C7−C8 1.357(9), C8−C1 1.442(8), C−C−C (mean) 135(2), P1−Ni−P2 91.3(2), P1,P2,Ni/C1,C2,Ni 13, (C1−C8)/C1,C2,Ni 93.

The midpoint of the C1−C2 bond is coplanar with Ni, P1, and P2 (±0.06 Å), giving the metal a *TP*-3 coordination geometry, and the coordinated double bond is only slightly twisted out of the plane (13°), thus enabling good backbonding from the metal.[28]

In the (d^tbpe)Ni complex **1b** (Figure 4) the COT ring is also planar. The largest deviation from a least-squares plane through all carbon atoms is ±0.03 Å and thus even less than for **1a** and close to the corresponding value in the aromatic dianion COT^{2-} (±0.005 Å).[11b] Here again C−C bond lengths are found to be alternating [C═C_{mean} 1.36(2), C−C_{mean} 1.43(1) Å]. The coordinated double bond of the COT is elongated to 1.407(4) Å and is similar to that in **1a**. Inspection of the packing of the molecules in the unit cell reveals that the planarity of the COT ligand is not induced by packing forces since the shortest intermolecular distances are between *tert*-butyl groups located on the phosphorus ligands (3.43 Å), whereas intermolecular contacts involving atoms of the COT group are larger than 3.64 Å. The bending of the COT ring plane from the metal [(C1−C8)/C1,C8,Ni 98°] is somewhat larger than for **1a**, but the twist of the coordinated C═C bond out of the Ni coordination plane (P1,P2,Ni/C1,C8,Ni 10°) is smaller.

As compared with **1a,b**, the angle between the plane through the Ta atom and the coordinated C═C bond and the plane of the COT ring (±0.02 Å) in $Cp_2Ta(n\text{-}C_3H_7)(\eta^2\text{-}C_8H_8)$[13] is distinctly larger (116°). The C═C bond coordinated to Ta is unexpectedly long [1.45(2) Å] and the C−C bond alternation in the uncoordinated part of the ring is less regular, though this may be due to the relatively poor refinement of the structure (R = 9.9%).

{(^{i}Pr$_2$PC$_2$H$_4$P^{i}Pr$_2$)Ni}$_2$\{μ-η^4(1,2,5,6):η^4(3,4,7,8)-C$_8$H$_8$\} (2a) and {(^{t}Bu$_2$PC$_2$H$_4$P^{t}Bu$_2$)Ni}$_2$(μ-η^2:η^2-C$_8$H$_8$) (2b). Mononuclear **1a** reacts with the equimolar amount of (d^ippe)Ni(η^2,η^2-C_6H_{10}) in diethyl ether solution upon gentle heating (40 °C) with displacement of the 1,5-hexadiene ligand to afford large *orange* cubes of the dinuclear derivative **2a**·Et_2O in 60% yield (eq 2a). The crystals disintegrate at ambient temperature to a yellow orange powder due to the loss of the solvent molecule. Similarly, complex **1b** reacts (20 °C) with a half-equiv of {(d^tbpe)Ni}$_2$(μ-C_6H_6)[14,17] [but not with (d^tbpe)Ni(C_2H_4)] to yield *red brown violet* microcrystals of **2b** in 75% yield (eq 2b).

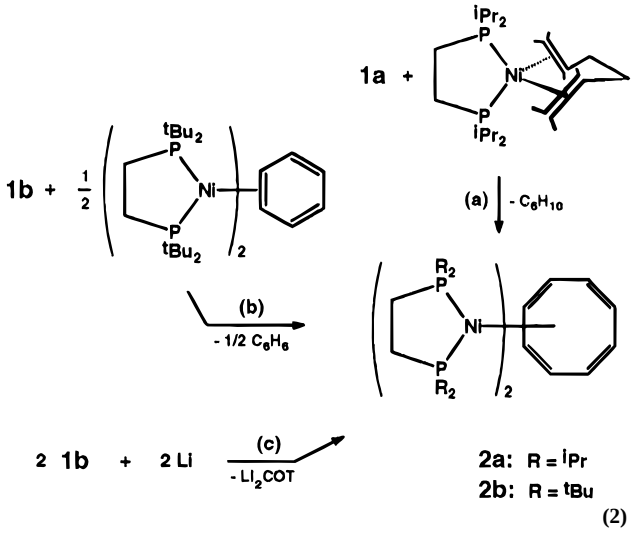

(2)

Complex **2b** can also be prepared by stirring an ethereal suspension of **1b** and lithium powder for 30 min at 20 °C (44%; eq 2c).[29] Further reaction of **2b** and also the reaction of **1a** with lithium give rise to a mixture of unidentified products. When COT is added to the orange solution (THF-d_8) of dinuclear **2a**, the color immediately turns dark red, and mononuclear **1a** is formed quantitatively (NMR). In contrast, dinuclear **2b** has to be dissolved in neat COT to allow for a complete formation of mononuclear **1b** (in about 1 h). Thus, the mono- and dinuclear complexes are subjected to the equilibrium

$$2\mathbf{1a,b} \rightleftharpoons \mathbf{2a,b} + \mathrm{COT}$$

which in the presence of COT lies completely on the side of **1a,b**. The slow formation of **1b** is presumably due to kinetic reasons. As will be shown below from the solid-state ^{13}C and ^{31}P NMR spectra, complex **2b** forms two isomers. These are designated C_2-**2b** and C_i-**2b** on the basis of their presumed symmetry. While C_2-**2b** preferentially crystallizes at low-temperature (70%), the solid completely converts into C_i-**2b** upon warming to 40 °C (eq 3). The conversion is reversible upon dissolution.

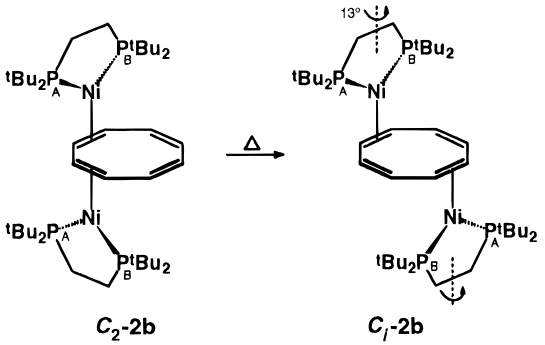

Complexes **2a,b** are only slightly soluble in diethyl ether (20 °C) but can be recrystallized from this solvent. THF appears to be the best solvent for all the complexes, but the solubilities of dinuclear **2a,b** are nevertheless distinctly lower than those of mononuclear **1a,b**. Complexes **2a** (mp 161 °C) and (C_i-)**2b** (mp 225 °C) are thermally very stable. In the mass spectra the

(28) Rösch, N.; Hoffmann, R. *Inorg. Chem.* **1974**, *13*, 2656.

(29) The method of partial reductive removal of COT from Ni(0) to form a dinuclear complex with a bridging COT ligand has previously been used for the synthesis of {(Ph_4C_4)Ni}$_2$(μ-C_8H_8). Fröhlich, C.; Hoberg, H. *J. Organomet. Chem.* **1981**, *204*, 131.

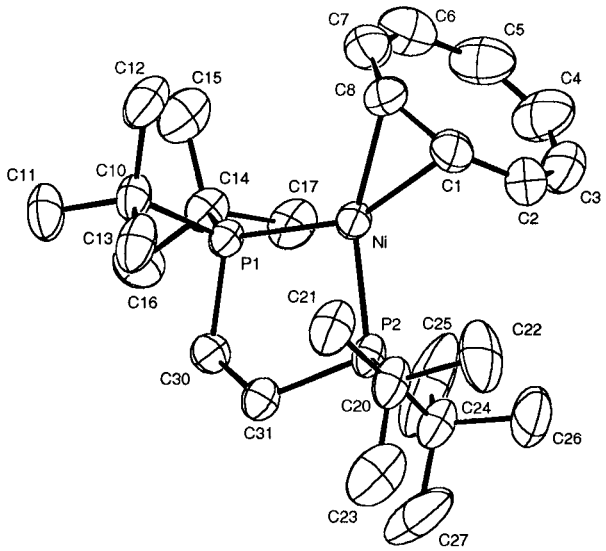

Figure 4. Molecular structure of complex **1b**. Selected bond distances (Å): Ni−P1 2.207(1), Ni−P2 2.208(1), Ni−C1 2.023(2), Ni−C8 2.037(2), C1−C8 1.407(4), C1−C2 1.444(4), C2−C3 1.364(5), C3−C4 1.421(6), C4−C5 1.328(6), C5−C6 1.427(6), C6−C7 1.362(5), C7−C8 1.439(4). Selected angles (deg): C−C−C (mean) 135(1), P1−Ni−P2 92.5(2), P1,P2,Ni/C1,C8,Ni 10, (C1−C8)/C1,C8,Ni 98.

molecular ions are observed (**2a**: *m/e* 744, 3%; **2b**: 856, 1%). These expel the [(d^{i}ppe)Ni] or [(d^{t}bpe)Ni] moiety to give the molecular ions of **1a** and **1b,** respectively. In the IR spectrum of **2a** and C_i-**2b** no bands are observed between 1600 and 1500 cm^{-1}.[30] C_i-**2b** exhibits its highest frequency COT ring-stretching mode as a *strong* band at 1476 cm^{-1}, while **2a** displays it only as a *weak* absorption[20,31a] at 1465 cm^{-1} (forming a small shoulder of a phosphine ligand band). Further prominent bands of the μ-COT ligands of **2a** (1332, 1100, 643 cm^{-1}) and C_i-**2b** (1425, 1286, 705 cm^{-1}) differ significantly, suggesting different binding modes of the complexes.

Solution and Solid-State NMR Spectra of 2a. In the solution ^{1}H and ^{13}C NMR spectra (27 °C) of **2a**, the COT ligand gives rise to single sharp resonances which display resolved couplings to the phosphorus nuclei (some line broadening with depletion of the couplings is observed at −80 °C). As compared with **1a,b**, the COT ligand complexation shifts[32] are increased still further [$-\Delta\delta_H$ = 1.3 ppm, $-\Delta\delta_C$ = 42 ppm], but the coupling constant *^1J(CH) has reverted to that of free COT* (154.5 Hz). The magnitude of ^1J(CH) agrees well with that of complexes in which the four C═C bonds of an *olefinic* (nonplanar) COT ligand are chelating two *T*-4 Ni(0) centers, as is also the case for {(RN═CHCH═NR)Ni}$_2$(μ-η^4:η^4-COT) (R = C_6H_3-2,6-^{i}Pr$_2$)[33] (Table 1). Thus, all C═C bonds in **2a** are coordinated, and the structure is static (see Figure 6).

The ^{13}C and ^{31}P CP-MAS NMR spectra (24 °C) of **2a** (Figure 5) agree well with the solution NMR spectra with the qualification that they indicate lower symmetry (C_1; cf. X-ray, D_2).[34] Thus, the COT ligand displays six close ^{13}C resonances [δ_C 92.3, 91.3, 90.7, 89.2 (triple degenerate), 87.9, 87.0] centered at δ_C 89.6 (solution NMR: δ_C 90.3) (Figure 5a). For the PC*H*Me$_2$ groups of the d^{i}ppe ligands, several signals overlap ($\delta_C \approx 25$) and have not been further interpreted but for the PCH*Me*$_2$ groups 11 (of expected 16) resonances are resolved. The PCH*Me*$_2$ region of the spectrum has been simulated by the Bruker GLINFIT program and by using 16 Lorentz lines of nearly equal intensity and line width, an excellent agreement (7% TMS error) with the observed spectrum was achieved (Figure 5b,c). The PCH$_2$ resonances (four expected at $\delta_C \approx$ 21) are apparently overlapped by the PCH*Me*$_2$ signals. The ^{31}P nuclei of both d^{i}ppe ligands give rise to two AB spin systems (δ_P 67.0, 65.3 and 63.0, 62.0), which display the couplings *J*(PP) = 36 ± 5 and 28 ± 5 Hz, respectively, as determined by *J*-resolved 2D ^{31}P NMR (Figure 5d).

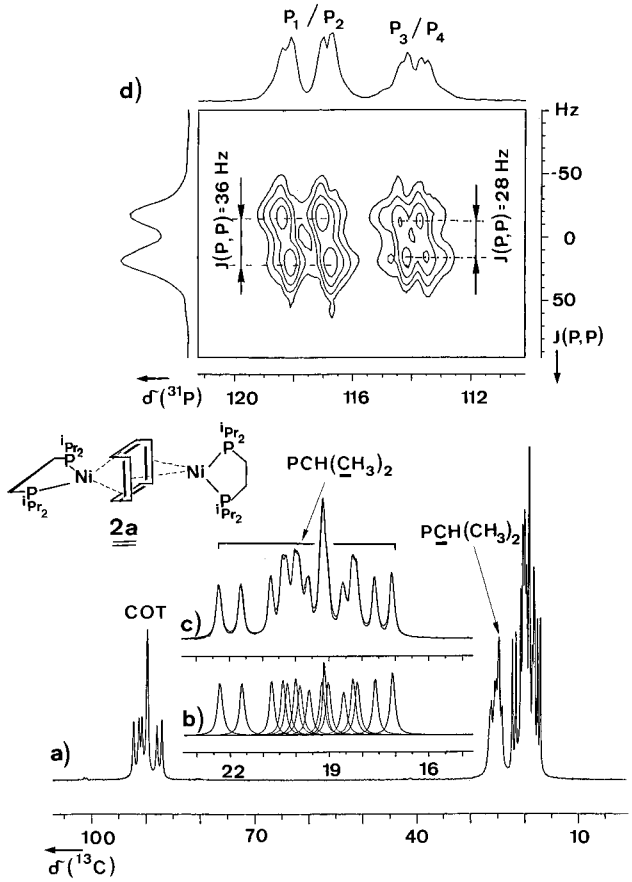

Figure 5. ^{13}C CP-MAS TOSS NMR spectrum of **2a** (trace a). The PCH*Me*$_2$ region of the ^{13}C NMR spectrum *without* side-band suppression (trace c, lower line) is compared with the simulated spectrum (trace c, upper line), calculated from 16 Lorentzian lines (trace b). Isotropic part of *J*-resolved 2D ^{31}P CP-MAS NMR spectrum of **2a** (trace d). For two AB spin systems (resulting from two independent d^{i}ppe ligands) different coupling constants *J*(PP) are found.

Crystal Structure of 2a·Et$_2$O. The molecular structure of **2a**, which crystallizes as a 1:1 cocrystal with Et$_2$O, is depicted in Figure 6. The complex displays a central tub-shaped μ-*trans*-η^4(1,2,5,6):η^4(3,4,7,8)-COT ligand coordinated by two *T*-4 [(d^{i}ppe)Ni(0)] groups. This type of COT coordination is not uncommon [e.g., (AgNO$_3$)$_3$(μ-COT)$_2$,[35] (CpCo)$_2$(μ-COT),[31b] and {CpRh}$_2$(μ-COT)[31b,36]]. Complex **2a** exhibits noncrystallographic D_2 symmetry with three approximate 2-fold axes,

(30) Weak absorptions at 1595 and 1556 cm^{-1} may possibly be attributed to C_2-**2b**.

(31) (a) Fritz, H. P.; Keller, H. *Z. Naturforsch., B: Anorg. Chem., Org. Chem.* **1961**, *16*, 348. (b) Paulus, E.; Hoppe, W.; Huber, R. *Naturwissenschaften* **1967**, *54*, 67.

(32) Jolly, P. W.; Mynott, R. *Adv. Organomet. Chem.* **1981**, *19*, 257.

(33) Bonrath, W.; Pörschke, K.-R.; Michaelis, S. *Angew. Chem.* **1990**, *102*, 295; *Angew. Chem., Int. Ed. Engl.* **1990**, *29*, 298.

(34) It is a frequently encountered phenomenon that in the solid state CP-MAS NMR spectra of complexes of this kind the apparent symmetry of the static parts of the complexes is C_1, disregarding possible ligand dynamics and disregarding a higher idealized symmetry of the complexes as determined by solution NMR or X-ray structure analysis. The reduction of symmetry to C_1 is thought to be caused by subtle differences in the environment of the nuclei which are concealed by other methods but become discernible by solid state NMR.[17] See also: Wu, G.; Wasylishen, R. E. *Inorg. Chem.* **1996**, *35*, 3113 and references cited therein.

(35) Mak, T. C. W. *J. Organomet. Chem.* **1983**, *246*, 331.

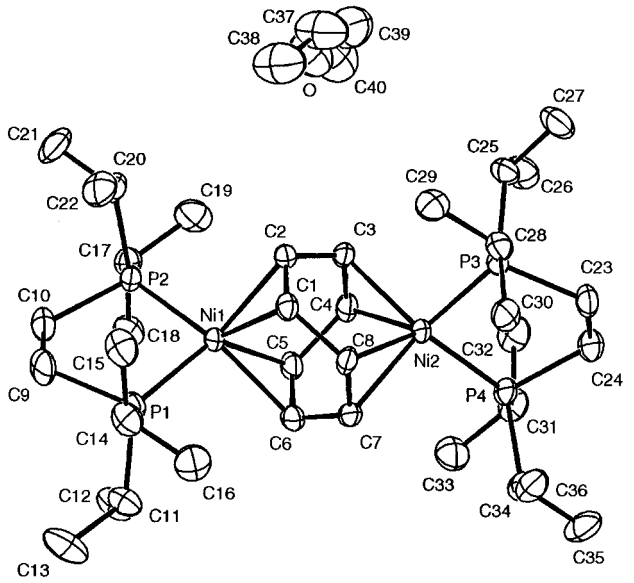

Figure 6. Molecular structure of complex **2a·Et$_2$O**. Selected bond distances (Å): Ni1···Ni2 3.878(1), Ni1−P1 2.173(1), Ni1−P2 2.173(1), Ni2−P3 2.172(1), Ni2−P4 2.170(1), Ni1−C1 2.124(3), Ni1−C2 2.110(3), Ni1−C5 2.117(3), Ni1−C6 2.108(3), Ni2−C3 2.114(3), Ni2−C4 2.124(3), Ni2−C7 2.112(3), Ni2−C8 2.116(3), C1−C2 1.383(5), C2−C3 1.485(6), C3−C4 1.386(5), C4−C5 1.504(5), C5−C6 1.395(5), C6−C7 1.497(5), C7−C8 1.390(5), C8−C1 1.504(5). Selected angles (deg): P1−Ni1−P2 91.00(4), P3−Ni2−P4 90.84(4), P1,P2,Ni1,Ni2/P3,P4,Ni2,Ni1 79, C−C−C (mean) 119.3(3).

running along the Ni···Ni vector and through the midpoints of the bonds C1−C8, C4−C5 and C2−C3, C7−C8. Owing to a distortion of the molecule from idealized D_{2d} symmetry, presumably as a result of inherent asymmetry of the d^{i}ppe ligand, the coordination geometry around the Ni atoms is not exactly tetrahedral, and the mean plane through P1,P2,Ni1,Ni2 makes an angle of 79° to that through P3,P4,Ni2,Ni1. C−C distances within the bridging COT ring reflect the individual characters of the bonds. Thus, the C═C bond distances of the coordinated double bonds C1−C2, C3−C4, C5−C6, and C7−C8 [mean, 1.389(5) Å] are significantly shorter than the adjoining C−C single bonds [mean, 1.498(9) Å] but longer than those of the free ligand.

Solution and Solid-State NMR Spectra of 2b. In the solution ^{1}H and ^{13}C NMR spectra of **2b** (27 °C) the COT ligand gives rise to sharp singlets. At −80 °C these resonances are broad. The NMR spectra indicate that the structure of **2b** is dynamic in solution, and an exchange of coordinated and uncoordinated COT C═C bonds takes place by a mechanism similar to that depicted for **1a,b** in Figure 1a.[37] The COT ligand mean complexation shifts (the time average for coordinated and uncoordinated C═C bonds) are of the same magnitude as for **2a**, but the mean coupling constant *^1J(CH) is reduced to 147 Hz* as compared with the value for **1a,b**, and in contrast to **2a** (Table 1). A comparison of the low-temperature spectra of **1a,b** and **2b** suggests that the structural dynamics of dinuclear **2b** are markedly slower than those of the mononuclear complexes. Hence, it appears the exchange process in solution is slowest for **2b** (largest activation energy) and fastest for **1a** (lowest activation energy).

Concomitant with an increased ^{13}C NMR shielding of the COT ligand in the dinuclear complexes **2a,b** as compared with the mononuclear complexes **1a,b**, the ^{31}P NMR signals are shifted also to high-field. In fact, for **2b** this is by 13.9 ppm and for **2a** by 16.2 ppm (Table 1). Apparently, in the dinuclear complexes **2a,b** the total charge transfer to the COT ligand is larger, but the contribution of each [($R_2PC_2H_4PR_2$)Ni(0)] fragment is smaller, and more electron density remains at the phosphorus atoms as compared with the situation in mononuclear **1a,b**.[38]

The exceedingly low (mean) coupling constant ^1J(CH) as well as the intense color suggests the presence of a semiaromatic planar COT ligand. Futher information on the coordination mode of the COT ligand is obtained from the solid-state ^{13}C and ^{31}P CP-MAS NMR spectra. According to these, freshly isolated **2b** comprises an approximate 70:30 mixture of two isomers, designated here as C_2-**2b** and C_i-**2b**. For isomer C_2-**2b** (Figure 7a) two broad signals (presumably unresolved pairs) of the ^{13}C atoms of two uncoordinated C═C bonds (δ_C 122.0, 119.8) and one (presumably 4-fold degenerate) signal of the ^{13}C atoms of two coordinated C═C bonds (δ_C 55.8) are observed (mean: δ_C 88.4). The d^{t}bpe ligands give rise to three broad P*C*Me$_3$ signals [δ_C 35.9, 35.2 (degenerate), 34.9], three broad PC*Me*$_3$ signals [δ_C 32.7, 31.5 (degenerate), 31.1] (four signals each are expected for one d^{t}bpe ligand), and an unresolved signal for P_ACH_2 and P_BCH_2 (δ_C 24.6).[34] The ^{31}P spectrum (Figure 7b) displays two overlapping AB spin systems at δ_P 75.7, 73.7 for which similar couplings J(PP) = 110 ± 5 Hz have been determined from the *J*-resolved 2D spectrum. Accordingly, isomer C_2-**2b** is proposed to consist of two *TP*-3 [(d^{t}bpe)Ni(0)] moieties coordinated antifacially to *adjacent* C═C bonds of the semiaromatic COT ring. The structure is static in the solid, i.e., neither a rotation of the COT ring nor a rotation of the [(d^{t}bpe)Ni(0)] moieties about the C═C bond axis occurs. The binding situation in C_2-**2b** is similar to that in {(d^{t}bpe)Ni}$_2$(μ-C_6H_6) [J(PP) = 105 ± 5 Hz], whose structure has been determined by X-ray crystallography.[17] The relatively large coupling J(PP) seems to indicate a high charge at the Ni(0) center.[17]

C_i-**2b** is best studied after tempering the crude product at 40 °C, whereupon it is the only isomer present (eq 3). For the COT ligand of C_i-**2b** a pair of signals for two uncoordinated (δ_C 122.9, 121.7) and two coordinated C═C bonds (δ_C 55.5, 54.4) are observed (mean: δ_C 88.6) (Figure 7c). The d^{t}bpe ligands give rise to two broad P*C*Me$_3$ signals (δ_C 36.5, 34.6), an unresolved signal for (two types of chemically different) PC*Me*$_3$ groups (δ_C 32.2), and a broad signal for PCH_2 (δ_C 23.8). According to the ^{13}C NQS spectrum, the COT ligand is nonfluxional. In the solid-state ^{31}P spectrum (Figure 7d) one broad signal (δ_P 77.0; presumably unresolved AB spin systems)[34] is observed. Although the spectra are not fully resolved, they are consistent with a higher point symmetry than that of C_2-**2b** and are attributed to a complex in which two *TP*-3 [(d^{t}bpe)Ni(0)] moieties are coordinated antifacially to *trans-annular* C═C bonds of the semiaromatic COT ring, as has been found by X-ray structure analysis (see Figure 8).

Crystal Structure of C_i-2b. The single crystal X-ray diffraction analysis of C_i-**2b** (Figure 8) shows a transannular coordination of the COT ring by two *TP*-3 [(d^{t}bpe)Ni(0)] groups. The molecule crystallizes about an exact center of symmetry located at the middle of the C_8 ring; the molecular point symmetry is thus C_i.

The C_8 ring in C_i-**2b** is planar (rms deviation 0.01 Å), as observed for **1a,b** but in strong contrast to **2a**, where the central

(36) Brenner, K. S.; Fischer, E. O.; Fritz, H. P.; Kreiter, C. G. *Chem. Ber.* **1963**, *96*, 2632. Bieri, J. H.; Egolf, T.; von Philipsborn, W.; Piantini, U.; Prewo, R.; Ruppli, U.; Salzer, A. *Organometallics* **1986**, *5*, 2413.

(37) The C═C bond exchange in **2b** according to Figure 1a proceeds as a concerted motion of the nickel atoms at opposite faces of the COT ligand. An exchange mechanism according to Figure 1b is precluded as long as the Ni atoms are coordinated to transannular C═C bonds.

(38) The reverse effect is observed for the corresponding benzene complexes.[14,17]

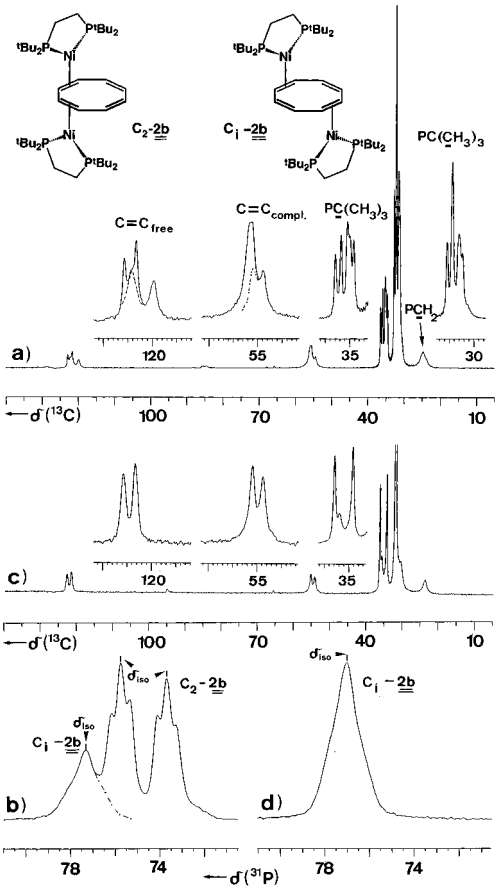

Figure 7. ^{13}C TOSS CP-MAS (traces a, c) and ^{31}P CP-MAS NMR spectra (traces b, d; only isotropic part) of **2b**. Freshly prepared **2b** consists of a mixture of two isomers, designated as C_2-**2b** and C_i-**2b** (traces a, b). After tempering the sample several hours at 40 °C, only one isomer (C_i-**2b**) is detected by solid-state NMR (traces c, d).

COT ligand has a tub conformation. The bond distances within the C_8 ring are significantly different from one another, indicating substantial localization of the C═C bonds. The shortest distance is between C3 and C4 [1.355(6) Å], consistent with an uncoordinated C═C bond. The C1−C2 bond [1.411(6) Å] is markedly longer because of its coordination to the Ni atom, while the interlinking bonds at C2−C3 [1.430(6) Å] and C4−C1* [1.447(6) Å] are still longer.

The coordinated C−C bonds are slightly twisted out of the Ni coordination plane (P1,P2,Ni/C1,C2,Ni 13°) (**1a**, 13°; **1b**, 10°), whereby C1, C2, Ni, and P1 are coplanar (±0.01 Å), and P2 lies 0.5 Å out of this plane. The coordination of two Ni moieties to the COT ring instead of one (**1a,b**) results in an increased angle between the plane of the C_8 ring and a plane defined by one Ni atom and the two C atoms of the coordinated C═C double bond. In **2b** this angle is 106°, whereas in **1b** (same d^{t}bpe ligand) the equivalent angle is 98°. Concomitant with this change the distance of the coordinated C═C bond in **2b** (C1−C2 [1.411(6) Å]) is slightly longer than for **1b** (C1−C8 [1.407(4) Å]), although the difference is hardly significant (1σ). We presume that the changes in the angle and the bond distance reflect an increased p character (sp^3) of the coordinated C atoms in going from **1b** to **2b**.

Discussion

The present study provides a systematic characterization of Ni(0) complexes with the COT ligand in the semiaromatic as well as olefinic forms. The binding modes of the COT ligands give important information about the properties of the mono-

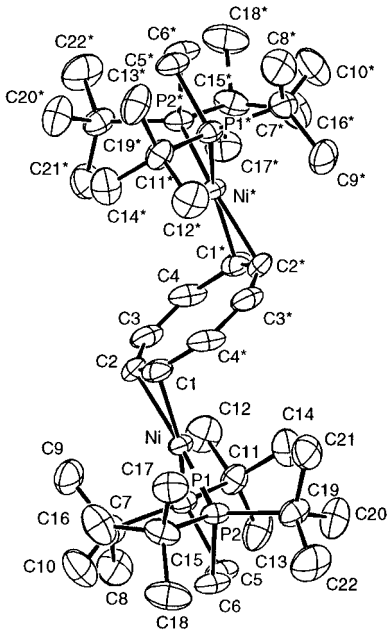

Figure 8. Molecular structure of C_i-**2b**. Selected interatomic distances (Å) and angles (deg): Ni−P1 2.190(1), Ni−P2 2.183(1), Ni−C1 2.023(4), Ni−C2 2.020(4), C1−C2 1.411(6), C1−C4* 1.447(6), C2−C3 1.430(6), C3−C4 1.355(6), C−C−C(mean) 135(1), P1−Ni−P2 93.47(4), P1,P2,Ni/C1,C2,Ni 13, (C1−C4, C1*−C4*)/C1,C2,Ni 106.

(**1a,b**) and dinuclear (**2a,b**) complexes of Ni(0) containing simultaneously phosphines and COT.

For mononuclear **1a,b** an η^2-coordinated semiaromatic COT ligand has been established by X-ray structure analysis, as observed previously only for $Cp_2Ta(n\text{-}C_3H_7)(\eta^2\text{-}C_8H_8)$.[13] The complexes are very intensively colored (Ni: dark violet; Ta: dark red). In the IR spectrum the COT ligands give rise to three prominent C═C stretching bands in the region of 1600−1470 cm^{-1}, the central band at 1535 ± 20 cm^{-1} being the most intense. The coordination of the η^2-COT ligand of the 16e Ni(0) complexes is dynamic even in the solid, and the low-temperature solution and ambient temperature solid-state NMR data represent mean values for the coordinated und uncoordinated -CH═CH- moieties. The *averaged* ^{1}H and ^{13}C NMR COT ligand complexation shifts[32] are $-\Delta\delta_H \approx 1.1-1.2$ ppm and $-\Delta\delta_C \approx 28$ ppm, while the *averaged* coupling constant ^1J(CH) is reduced (from that of uncoordinated COT by about 5.5 Hz) to ≈149 Hz (Table 1). From a comparison with the NMR data of uncoordinated COT and the solid-state NMR data of **2b**, the ^{1}H and ^{13}C NMR resonances of the *coordinated C*═C bond of **1a,b** in the *static structure* can be expected to be at rather high field ($\delta_H < 2.0$, $\delta_C < 70$), and the corresponding coupling constant is expected to be extremely small [^1J(CH) ≪ 147 Hz].[39]

It appears that strong backbonding from the metal center to the COT ligand is a prerequisite for achieving the semiaromatic η^2-COT coordination. In the case of the Ta complex this criterion is satisfied by the d^2 Ta(III) configuration, while at the same time the 18e shell precludes a higher COT hapticity than two. For nickel, various 18e *T*-4 d^{10} Ni(0) complexes L_2Ni(COT) containing a chelating *olefinic* η^4(1,2,5,6)-COT ligand are known. Examples are $(Me_3P)_2$Ni{η^4(1,2,5,6)-COT} (preliminary X-ray analysis),[40] $(Me_2PC_2H_4PMe_2)$Ni{η^4(1,2,5,6)-COT},[40] and (RN═CHCH═NR)Ni{η^4(1,2,5,6)-COT} (R = C_6H_3-2,6-^{i}Pr$_2$)[33].[41] *T*-4 d^{10} Ni(0) is relatively weakly back-

(39) Cf.: (d^{t}ppe)Ni(C_2H_4): δ_H 1.82, δ_C 33.4, ^1J(CH) = 152 Hz.[14,16]
(40) Pörschke, K.-R.; Goddard, R.; Krüger, C. Unpublished.
(41) In the *T*-4 Ni(0) complexes L_2Ni{η^2(1,2,5,6)-COT} the uncoordinated C═C bonds of the COT ligand give rise to a strong IR absorption band near 1620 cm^{-1}.

bonding, and in the presence of the 1,4-diazabutadiene ligand the chelating COT coordination mode is maintained in spite of the bulk of the ligand. The situation turns out to be different for phosphine ligands, which are stronger electron donors than 1,4-diazabutadienes. Here, increasing the bulk of the substituents R in the sequence Me < ^{i}Pr < ^{t}Bu destabilizes the *T*-4 geometry in favor of the *TP*-3 geometry. In complexes ($R_2PC_2H_4PR_2$)Ni(COT) for R = ^{i}Pr a change of the COT coordination mode from chelating to η^2-COT is thereby induced. The emerging *TP*-3 d^{10} Ni(0) center exhibits a much improved backbonding and causes the η^2-COT ligand to adopt a *semiaromatic* rather than an olefinic character, as evidenced by the planarity of the ring. Thus, in **1a,b** the combination of steric and electronic effects accounts for the semiaromatic η^2-COT coordination at a coordinatively unsaturated 16e Ni(0) center.

When a second [(d^{t}bpe)Ni(0)] fragment is coordinated to the semiaromatic COT ligand in **1b** to give dinuclear **2b**, the color of the (solid) complex lightens slightly to red brown violet. The initially obtained product consists of two isomers which according to the presumed antifacially adjacent or transannular coordination of the [(d^{t}bpe)Ni(0)] fragments to the COT ring are designated C_2-**2b** and C_i-**2b**; the structure of the latter isomer has been determined by X-ray analysis. In the IR spectrum of C_i-**2b** one strong band at 1476 cm^{-1} (instead of the three C═C bands of **1a,b**) is observed. The structure of **2b** is dynamic in solution due to an exchange of coordinated and uncoordinated C═C bonds, but it is static in the solid-state. While the (averaged) solution ^{1}H and ^{13}C resonances of the COT ligand are shifted further to high field ($-\Delta\delta_H$ = 1.4 ppm, $-\Delta\delta_C$ = 42 ppm) as compared with **1b**, the (averaged) coupling constant ^1J(CH) is still further reduced (147 Hz). Thus, there is a steady shift of the ^{13}C COT resonance to higher field and a steady *decline* in ^1J(CH) in going from COT to **1a,b** to **2b** to Li_2/K_2-COT (Table 1). We conclude from these properties that the character of the COT ring in **2b** (Figure 8) is still *semiaromatic*, with a possible tendency toward the aromatic. The binding mode of the μ-η^2:η^2-COT ligand and its semiaromatic character is driven by the *TP*-3 geometry of the [(d^{t}bpe)Ni(0)] fragments.

The central COT ligand in dinuclear **2a** is tub-shaped, as revealed by crystal structure analysis, and two pairs of transannular C═C bonds chelate the antifacially coordinated *T*-4 [(d^{i}ppe)Ni(0)] fragments. Thus, the character of the COT ligand in **2a** is decidedly *olefinic*, which is also indicated by the light orange color of the complex and presence of only a weak IR C═C stretch absorption band below 1470 cm^{-1} (all C═C bonds are coordinated). In the NMR spectra the ^{1}H and ^{13}C complexation shifts of the COT ligand are as large as for **2b**, but the coupling constant ^1J(CH) coincides with that of uncoordinated COT, consistent with a *T*-4 Ni(0) alkene complex.[42]

The difference in the binding of the COT ligand in **2a** as compared with **1a,b** and in particular (C_i-)**2b** begs the question: Why does the semiaromatic COT ligand in **1a** revert upon coordination of the second [(d^{i}ppe)Ni(0)] fragment to an olefinic binding mode in dinuclear **2a**? To answer this question it is necessary to bear in mind that for dinuclear L_2Ni(0)-COT complexes (L_2, e.g., $2PR_3$, $R_2PC_2H_4PR_2$, RN═CHCH═NR) the tub-shaped μ-η^4(1,2,5,6):η^4(3,4,7,8)-COT coordination mode is generally the energetically most favorable. This is because its tub conformation is almost undistorted as compared with uncoordinated COT, and *all* C═C bonds are coordinated to metal centers. This coordination mode is, however, only adopted if a *T*-4 coordination geometry can be taken on by the Ni(0) center,[43] which is indeed the case for [(d^{i}ppe)Ni(0)] and most other [L_2Ni(0)] fragments, but not for [(d^{t}bpe)Ni(0)]. The olefinic μ-η^4(1,2,5,6):η^4(3,4,7,8)-COT coordination mode in **2a** can thus be considered to be the rule for dinuclear L_2Ni(0)-COT complexes. The semiaromatic COT-coordination modes in the isomers of **2b** represent an exception, imposed by the strict *TP*-3 configuration requirement of the (d^{t}bpe)Ni(0) moiety.

Finally, we would like to mention a possible connection of the results to the nickel-catalyzed cyclotetramerization reaction of ethyne to afford COT. For the mechanism of this reaction Reppe has envisaged an intermediate in which a C_8H_8 chain is coordinated by both ends to a central nickel atom.[44] According to current perception of the mechanisms of homogeneously catalyzed reactions this intermediate is likely to undergo C−C bond formation with ring-closure to produce a Ni-COT complex as the subsequent intermediate on the reaction profile (eq 4). Possibly, the mononuclear complexes **1a,b** and dinuclear (C_i-)**2b** represent model complexes of such an intermediate.

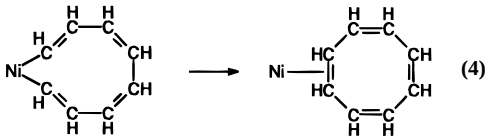

(4)

Experimental Section

All reactions and manipulations were performed using Schlenk-type techniques under an inert atmosphere of argon. Solvents were dried by destillation from $NaAl(C_2H_5)_4$. (d^{i}ppe)Ni(C_2H_4), (d^{i}ppe)Ni(η^2,η^2-C_6H_{10}),[15] (d^{t}bpe)Ni(C_2H_4),[16] and {(d^{t}bpe)Ni}$_2$(μ-C_6H_6)[14,17] were prepared as reported. COT was a gift from BASF AG. Microanalyses were performed by the Mikroanalytisches Labor Kolbe, Mülheim, Germany. ^{1}H NMR spectra (δ relative to internal TMS) were measured at 200, 300, and 400 MHz, ^{13}C NMR spectra (δ relative to internal TMS) at 50.3, 75.5, and 100.6 MHz, and ^{31}P NMR spectra (δ relative to external 85% aqueous H_3PO_4) at 81, 121.5, and 162 MHz on Bruker AM-200, WM-300, and AMX-400 instruments. Solvent for solution NMR was THF-d_8. EI mass spectra were recorded at 70 eV on a Finnigan MAT 95 and IR spectra on a Nicolet 7199 FT-IR instrument. Solid-state ^{13}C and ^{31}P CP-MAS NMR spectra were recorded on a Bruker MSL-300 spectrometer; experimental conditions were as described.[17]

Preparation of (^{i}Pr$_2$PC$_2$H$_4$P^{i}Pr$_2$)Ni(η^2-C$_8$H$_8$) (1a). COT (2 mL) is added to solid (d^{i}ppe)Ni(C_2H_4) (349 mg, 1.00 mmol) or (d^{i}ppe)Ni(η^2,η^2-C_6H_{10}) (403 mg, 1.00 mmol) at 20 °C. Upon stirring the complex dissolves to afford a dark red solution which changes color to brown when diethyl ether (10 mL) is added. Upon cooling to −78 °C fine violet needles precipitate; yield 340 mg (80%); mp 168 °C. MS (105 °C) *m/e* 424 (M^+, 38), 320 [(d^{i}ppe)Ni]$^+$, 100). IR (KBr) 2999 (═C−H), 1591, 1533 (C═C uncoordinated), 1485 (C═C coordinated), 667, 652 cm^{-1}. ^{1}H NMR (400 MHz, 27 °C) (for C_8H_8 see Table 1) δ 2.25 (m, 4H, $PCHMe_2$), 1.61 ("d", 4H, PCH_2), 1.16, 1.12 (each 12H, diastereotopic CH_3). ^{13}C NMR (100.6 MHz, 27 °C) (for C_8H_8 see Table 1) δ 27.4 (4C, $PCHMe_2$), 21.7 (2C, PCH_2), 19.9 (t, J(PC) = 3 Hz), 19.1 ("s", each 4C, diastereotopic Me). ^{31}P NMR (81 MHz, 27 °C) see Table 1. ^{13}C CP-MAS NMR (75.5 MHz, 24 °C): δ 101.3, 100.9 (each 8C, COT), 28.8, 28.0, 27.1, 26.8, 26.4, 25.6, 25.1, 24.4 (each

(42) Compare the ^{13}C NMR parameters (THF-d_8) of -CH═CH- of the following compounds (cod = cyclooctadiene). Cod: δ_C 129.4, ^1J(CH) = 152.5 Hz; Ni(cod)$_2$: δ_C 90.4, ^1J(CH) = 160 Hz; (RN═CHCH═NR)Ni(cod) (R = C_6H_3-2,6-iPr_2):[33] δ_C 89.3, ^1J(CH) = 155 Hz; (d^{i}ppe)Ni(cod): δ_C 79.5, ^1J(CH) = 153 Hz.

(43) Back-donation is weaker in *T*-4 Ni(0) than in *TP*-3 Ni(0) complexes.[43a] For (d^{i}ppe)Ni(0) complexes already a moderately strong electron accepting ligand (e.g., ethene) will favor the *TP*-3 geometry. The *T*-4 geometry is adopted only when the substrate is weakly or moderately electron accepting *and* when it is structurally supported by a chelating binding mode of the substrate (e.g., 1,5-hexadiene, 1,5-cyclooctadiene). (a) Pörschke, K.-R.; Mynott, R. *Z. Naturforsch., B: Anorg. Chem., Org. Chem.* **1984**, *39*, 1565.

(44) Reppe, W.; Schlichting, O.; Klager, K.; Toepel, T. *Justus Liebigs Ann. Chem.* **1948**, *560*, 1.

(45) Sheldrick G. M. *SHELXS-86*, *Acta Crystallogr. A* **1990**, *46*, 467.

(46) Sheldrick G. M. *SHELXL-93*, *Program for Crystal Structure Refinement*; Universität Göttingen, 1993.

1C, P*C*Me$_2$), 23.3 (1C), 22.6 (1C), 22.2 (2C), 21.8 (2C), 21.1 (1C), 20.7 (1C), 20.0 (1C), 19.7 (1C), 19.0 (1C), 18.4 (2C), 17.9 (1C), 17.6 (1C) (PC*Me*$_2$); PCH$_2$ (4C) is obscured. The signals correspond to two independent molecules. ^{31}P CP-MAS NMR (121.5 MHz, 24 °C) see text. Anal. Calcd for $C_{22}H_{40}NiP_2$ (425.2): C, 62.15; H, 9.48; Ni, 13.80; P, 14.57. Found: C, 61.30; H, 9.31; Ni, 14.23; P, 15.11.

Preparation of (^{t}Bu$_2$PC$_2$H$_4$P^{t}Bu$_2$)Ni(η^2-C$_8$H$_8$) (1b). The synthesis is carried out as for **1a** by reacting (d^{t}bpe)Ni(C$_2$H$_4$) (405 mg, 1.00 mmol) with COT (2 mL, excess). The reaction is distinctly slower (30 min.). After addition of diethyl ether (40 mL) and cooling the solution to −78 °C large bluish purple needles crystallize which are separated from the mother liquor, washed twice with cold pentane, and dried under vacuum (20 °C); yield 375 mg (78%); mp 218 °C. MS (130 °C) *m/e* 480 (M$^+$, 14), 376 ([(d^{t}bpe)Ni]$^+$, 100). IR (KBr) 2996 (=C−H), 1602, 1553 (C=C uncoord.), 1490 (C=C coord.), 670, 651 cm^{-1}. ^{1}H NMR (400 MHz, 27 °C) (for C$_8$H$_8$ see Table 1) δ 1.80 (m, 4H, PCH$_2$), 1.32 (m, 36H, CH$_3$); at −100 °C (300 MHz) all signals are broadened and have lost the fine resolution. ^{13}C NMR (100.6 MHz, 27 °C) (for C$_8$H$_8$ see Table 1) δ 36.2 (4C, P*C*CH$_3$), 31.0 (12C, CH$_3$), 24.1 (2C, PCH$_2$); at −100 °C (75.5 MHz) the signal of the C$_8$H$_8$ ligand (δ 104.9) is broad. ^{31}P NMR (81 MHz, 27 °C) see Table 1. ^{13}C CP-MAS NMR (75.5 MHz, 24 °C) and ^{31}P CP-MAS NMR (121.5 MHz, 24 °C) see text. Anal. Calcd for $C_{26}H_{48}NiP_2$ (481.3): C, 64.88; H, 10.05; Ni, 12.19; P, 12.87. Found: C, 64.79; H, 10.10; Ni, 12.11; P, 12.96.

Preparation of {(^{i}Pr$_2$PC$_2$H$_4$P^{i}Pr$_2$)Ni}$_2$(μ-η^4(1,2,5,6):η^4(3,4,7,8)-C$_8$H$_8$} (2a). A dark brown suspension of **1a** (850 mg, 2.00 mmol) in diethyl ether (20 mL) is combined with a yellow ethereal solution (20 mL) of (^{i}Pr$_2$PC$_2$H$_4$P^{i}Pr$_2$)Ni(η^2,η^2-C$_6$H$_{10}$) (806 mg, 2.00 mmol). The mixture is heated to 40 °C for 20 min and stirred at 20 °C for 1 day. Thereby the color changes to dark red. Upon cooling to −30 °C orange cubes of **2a**·Et$_2$O form, which are separated from the mother liquor, washed twice with pentane, and dried under vacuum at −30 °C. Drying at ambient temperature results in loss of the ether molecule to afford **2a** as a yellow orange-powder; yield 900 mg (60%); mp 161 °C. MS (150 °C) *m/e* 744 (M$^+$, 3), 424 (**1a**$^+$, 15), 320 ([(d^{i}ppe)Ni]$^+$, 47). IR 3003, 1465, 1332, 1100, 781/71, 643, 592 cm^{-1}. ^{1}H NMR (400 MHz, 27 °C) (for C$_8$H$_8$ see Table 1) δ 2.08 (m, 8H, PCHMe$_2$), 1.39 ("d", 8H, PCH$_2$), 1.09, 1.06 (each 24H, diastereotopic CH$_3$). ^{13}C NMR (100.6 MHz, 27 °C) (for C$_8$H$_8$ see Table 1) δ 26.1 ("t", 8C, PCHMe$_2$), 21.6 ("t", 4C, PCH$_2$), 19.7 ("t", J(PC) = 3 Hz), 18.6 ("s", each 8C, diastereotopic Me). ^{31}P NMR (162 MHz, 27 °C) see Table 1. ^{13}C CP-MAS NMR (75.5 MHz, 24 °C) and ^{31}P CP-MAS NMR (121.5 MHz, 24 °C) see text. Anal. Calcd for $C_{36}H_{72}Ni_2P_4$ (746.2): C, 57.94; H, 9.72; Ni, 15.73; P, 16.60. Found: C, 57.76; H, 9.75; Ni, 15.85; P, 16.56.

Preparation of {(^{t}Bu$_2$PC$_2$H$_4$P^{t}Bu$_2$)Ni}$_2$(μ-η^2:η^2-C$_8$H$_8$) (2b). Method (a). A solution of **1b** (481 mg, 1.00 mmol) in diethyl ether (60 mL) is added to solid {(d^{t}bpe)Ni}$_2$(μ-C$_6$H$_6$) (416 mg, 0.50 mmol). The mixture is stirred at 20 °C (2 h) whereupon red brown violet microcrystals precipitate from a dark red solution. After completing the crystallization at −78 °C the complex is separated by filtration, washed with pentane, and dried under vacuum; yield 645 mg (75%). **Method (b).** A suspension of **1b** (481 mg, 1.00 mmol) and lithium (15 mg, excess) in diethyl ether (30 mL) is stirred at 20 °C until all **1b** is dissolved (30 min). After separation of the excess of lithium by filtration the solution is cooled to −78 °C to afford the microcrystalline precipitate which is isolated as described (a); yield 190 mg (44%); mp 225 °C. MS (200 °C) *m/e* 856 (M$^+$, 1), 480 (**1b**$^+$, 2), 376 ([(d^{t}bpe)Ni]$^+$, 25), 261 ([^{t}Bu$_2$PC$_2$H$_4$P^{t}Bu]$^+$, 100). IR 2983 (=C−H), 1476 (C=C coord), 1425, 1286, 705, 660, 643 cm^{-1}. ^{1}H NMR (400 MHz, 27 °C) (for C$_8$H$_8$ see Table 1) δ 1.62 (m, 8H, PCH$_2$), 1.27 (m, 72H, CH$_3$). ^{13}C NMR (100.6 MHz, 27 °C) (for C$_8$H$_8$ see Table 1) δ 35.4 (8C, P*C*CH$_3$), 31.1 (24C, CH$_3$), 23.9 (4C, PCH$_2$). ^{31}P NMR (162 MHz, 27 °C) see Table 1. ^{13}C CP-MAS NMR (75.5 MHz, 24 °C) and ^{31}P CP-MAS NMR (121.5 MHz, 24 °C) see text. Anal. Calcd for $C_{44}H_{88}Ni_2P_4$ (858.5): C, 61.56; H, 10.33; Ni, 13.67; P, 14.43. Found: C, 61.50; H, 10.51; Ni, 13.55; P, 14.49.

Crystal Structure Determination of 1a. A crystal (black plate) of dimensions 0.07 × 0.08 × 0.36 mm was used for X-ray crystallography. Preliminary examination and data collection were performed at 20 °C with Cu Kα radiation (λ = 1.54178 Å) on an Enraf-Nonius CAD4 diffractometer equipped with a graphite-incident beam monochromator. Crystal data: $C_{22}H_{40}NiP_2$, M_r = 425.2 g mol^{-1}, monoclinic, space group $P2_1/c$, a = 14.291(1), b = 15.634(1), c = 20.880(1) Å, β = 94.24(1)°, V = 4652.4(3) Å^3 , Z = 8, D_{calcd} = 1.21 g cm^{-3}, F(000) = 1840, μ(Cu Kα) = 25.0 cm^{-1}, ψ-scan absorption correction (t_{min}: 0.883, t_{max}: 1.000). A total of 9479 reflections, 7511 unique with $I > 2.0\sigma$(I), were obtained by using $\omega-2\theta$ scan technique with a scan rate of 1−5° min^{-1} (in ω). The structure was solved by SHELXS-86[45] and refined by SHELXL-93[46] (refinement of F^2) to a final R_1 = 0.046, wR = 0.134 (observed reflections).

Crystal Structure Determination of 1b. A crystal (black plate) of dimensions 0.18 × 0.39 × 0.46 mm was used for X-ray crystallography. Preliminary examination and data collection were performed at 20 °C with Cu Kα radiation (λ = 1.54178 Å) on an Enraf-Nonius CAD4 diffractometer as for **1a**. Crystal data: $C_{26}H_{48}NiP_2$, M_r = 481.3 g mol^{-1}, triclinic, space group $P\bar{1}$, a = 9.128(1), b = 11.016(1), c = 15.482(1) Å, α = 71.38(1), β = 77.02(1), γ = 66.18(1)°, V = 1341.3(1) Å^3, Z = 2, D_{calcd} = 1.19 g cm^{-3}, F(000) = 524, μ(Cu Kα) = 22.2 cm^{-1}, analytical absorption correction (t_{min}: 0.683, t_{max}: 0.887). A total of 5706 reflections, 5504 unique, 5133 observed with $I > 2.0\sigma(I)$, were obtained by using $\omega-2\theta$ scan technique with a scan rate of 1−5° min^{-1} (in ω). The structure was solved by SHELXS-86[45] and refined by SHELXL-93[46] (refinement of F^2) to a final R_1 = 0.048, wR = 0.126 (observed reflections).

Crystal Structure Determination of 2a·Et$_2$O. A crystal (orange prism) of dimensions 0.37 × 0.49 × 0.24 mm was used for X-ray crystallography. Preliminary examination and data collection were performed at −100 °C with Mo Kα radiation (λ = 0.71073 Å) on a Siemens SMART CCD diffractometer equipped with a graphite-incident beam monochromator (10 s/frame, ω step 0.3°; θ_{max} 34.3°). Crystal data: $C_{40}H_{82}Ni_2OP_4$, M_r = 820.4 g mol^{-1}, monoclinic, space group $P2_1/n$, a = 16.3504(4), b = 11.1760(2), c = 25.4026(6) Å, β = 104.890(1)°, V = 4486.0(2) Å^3, Z = 4, D_{calcd} = 1.22 g cm^{-3}, F(000) = 1784, μ(Mo Kα) = 10.1 cm^{-1}, analytical absorption correction (t_{min}: 0.663, t_{max}: 0.797). 51 902 measured, 16 826 unique reflections (R_{av} 0.12), 10 905 observed [$I > 2\sigma(I)$]. The structure was solved by heavy-atom methods using SHELXS-86[45] and refined by SHELXL-93[46] (refinement on F^2) to a final R_1 = 0.070, wR = 0.202 (observed reflections).

Crystal Structure Determination of C_i-2b. A crystal (red plate) of dimensions 0.14 × 0.28 × 0.35 mm was used for X-ray crystallography. Preliminary examination and data collection were performed at 20 °C with Mo Kα radiation (λ = 0.71069 Å) on an Enraf-Nonius CAD4 diffractometer equipped with a graphite-incident beam monochromator. Crystal data: $C_{44}H_{88}$ Ni_2P_4, M_r = 858.4 g mol^{-1}, triclinic, space group $P\bar{1}$, a = 8.164(1), b = 11.106(1), c = 14.377(1) Å, α = 102.37(1), β = 96.92(1), γ = 107.27(1)°, V = 1191.8(2) Å^3, Z = 1, D_{calcd} = 1.20 g cm^{-3}, F(000) = 468, μ = 9.52 cm^{-1}, no absorption correction. A total of 4736 measured reflections, 4460 unique (R_{av} 0.02), 3194 observed with $I > 2.0\sigma(I)$, were obtained using an $\omega-2\theta$ scan technique with a scan rate of 1−5° min^{-1} (in ω). The structure was solved by SHELXS-86[45] and refined using SHELXL-93[46] (refinement of F^2) to a final R_1 = 0.046, wR = 0.128 (observed reflections).

Acknowledgment. We would like to thank the Volkswagen-Stiftung and the Fonds der Chemischen Industrie for financial support. Dedicated to Professor Gerhard Herberich on the occasion of his 60th birthday.

Supporting Information Available: Tables of data collection information, anisotropic thermal parameters, atom coordinates, bond lengths and angles, and figures for **1a,b**, **2a,** and C_i-**2b** are available (28 pages). See any current masthead page for ordering and Internet access instructions.

JA964210G